A DECOMPOSITION MODEL FOR SCATTERERS CHANGE DETECTION IN MULTI-TEMPORAL SERIES OF SAR IMAGES

S. Lobry, F. Tupin*

LTCI, CNRS, Télécom ParisTech
Université Paris-Saclay
75013, Paris, France

L. Denis

Laboratoire Hubert Curien, UMR 5516 CNRS,
Université de Saint-Etienne and Télécom Saint-Etienne,
Saint-Etienne, France

ABSTRACT

This paper presents a method for strong scatterers change detection in synthetic aperture radar (SAR) images based on a decomposition for multi-temporal series. The formulated decomposition model jointly estimates the background of the series and the scatterers. The decomposition model retrieves possible changes in scatterers and the date at which they occurred. An exact optimization method of the model is presented and applied to a TerraSAR-X time series.

Index Terms— Multi-Temporal Synthetic Aperture Radar (SAR), Change detection, Image decomposition, TV, L0

1. INTRODUCTION

Numerous sensors are now acquiring regularly earth images. Among them, SAR sensors are particularly popular thanks to their all weather capacities, radiometric stability, orbit accuracy and interferometric potential. Recently launched sensors like Sentinel-1 of ESA will acquire in the next years long multi-temporal SAR series with a revisit time of 12 days. This data allows the development of new applications, like interest area survey for security, safety or urban management applications, but also requires the development of new and adapted processing tools.

In this paper we are interested in the survey of urban and human settlements areas and specially building time evolution. We will focus on the bright scatterers, characterizing building signatures in SAR amplitude data. We aim at proposing a new framework for their detection and the monitoring of their changes. In the past years many works have been devoted to the analysis of SAR time series. Taking into account the specific distributions of SAR data, a widespread approach relies on hypothesis tests (see [1, 2, 3] to cite only a few). One of the main problems in such methods is the huge variability of SAR data estimates leading to limited performances. To overcome such a drawback, the spatial regularity of the signal can be exploited either at the pixel neighborhood level [4] or at the patch level [5]. In this paper we propose to define a framework combining hypothesis tests and regularization models for target change monitoring in multi-temporal SAR series.

*Thanks to CNES for funding.

2. DECOMPOSITION MODEL FOR STRONG SCATTERERS CHANGE DETECTION

Given a multi-temporal stack of n SAR images: $\mathbf{v} = \{\boldsymbol{v_1}, \ldots, \boldsymbol{v_n}\}$, we aim to jointly estimate the underlying radiometries $\boldsymbol{u}$ and detect changes. We consider the following decomposition model to account for the presence of strong scatterers $\boldsymbol{s}$ on top of a smooth background $\boldsymbol{b}$:

$$\forall t,\, \forall i,\, u_{t,i} = b_i + s_{t,i}\,, \tag{1}$$

where the radiometry $u_{t,i}$ at pixel i and time t is modeled with a background component b_i that is time-invariant and a time-varying strong scatterer component $s_{t,i}$ which is present only for some pixels (i.e., $s_{t,i} = 0$ for many pixels i).

We consider solving both:

- an *estimation problem*: estimation of b_i and $s_{t,i}$ for all pixels, and
- a *detection problem*: detection of the presence of a strong scatterer at pixel i and of a possible change in the radiometry $s_{t,i}$ of that scatterer with time.

Note that we restrict our study to cases where changes only affect strong scatterers, i.e., we do not consider changes in the background areas.

We propose here a framework to jointly solve these two problems, with some simplifying assumptions in order to keep the approach tractable. We consider first the detection problem, which can be formulated as a hierarchical hypothesis test:

$$\begin{cases} \mathcal{H}_0 : & d_i = 0 \;\Leftrightarrow\; \forall t,\, s_{t,i} = 0 \quad \text{(no strong scatterer)} \\ \mathcal{H}_1 : & d_i = 1 \;\Leftrightarrow\; \exists t,\, s_{t,i} > 0 \quad \text{(a strong scatterer)}\,, \end{cases} \tag{2}$$

where d_i is an indicator variable equal to zero if no strong scatterer is present on top of the background b_i at pixel i, and equal to 1 otherwise. In the absence of strong scatterer (i.e., under $\mathcal{H}_0$), the component $s_{t,i}$ is necessarily zero at all dates t. In the case of the presence of a strong scatterer at pixel i, a change may be detected by considering the following sub-hypotheses:

$$\begin{cases} \mathcal{H}_{1a}: \quad d_i = 1 \text{ and } c_i = 0 \;\Leftrightarrow\; \exists r > 0,\, \forall t,\, s_{t,i} = r \\ \qquad\qquad\qquad\qquad \text{(constant strong scatterer)} \\ \mathcal{H}_{1b}: \quad d_i = 1 \text{ and } c_i = 1 \;\Leftrightarrow\; \exists r > 0,\, \exists t_c,\, \forall t, \\ \qquad\qquad t < t_c \Rightarrow s_{t,i} = 0 \\ \qquad\qquad t \geq t_c \Rightarrow s_{t,i} = r \qquad \text{(apparition)} \\ \qquad \text{or} \\ \qquad\qquad t < t_c \Rightarrow s_{t,i} = r \\ \qquad\qquad t \geq t_c \Rightarrow s_{t,i} = 0 \quad \text{(disappearance)} \end{cases} \tag{3}$$

By assuming that fluctuations due to speckle are close to independent between pixels and between dates, we can express the negative log-likelihood of each hypothesis based on the the negative log-likelihood $\ell(v, b, r)$ of a single observation:

$$\mathscr{L}_0(b_i) = \sum_t \ell(v_{t,i}, b_i, 0) \tag{4}$$

$$\mathscr{L}_{1a}(b_i, r) = \sum_t \ell(v_{t,i}, b_i, r) \tag{5}$$

$$\mathscr{L}_{1b}^{\text{app}}(b_i, r, t_c) = \sum_{t=1}^{t_c-1} \ell(v_{t,i}, b_i, 0) + \sum_{t=t_c}^{n} \ell(v_{t,i}, b_i, r) \tag{6}$$

$$\mathscr{L}_{1b}^{\text{dis}}(b_i, r, t_c) = \sum_{t=1}^{t_c-1} \ell(v_{t,i}, b_i, r) + \sum_{t=t_c}^{n} \ell(v_{t,i}, b_i, 0)\,, \tag{7}$$

where the negative log-likelihood $\ell(v, b, r)$ to account for speckle noise in amplitude SAR images can be Rayleigh distribution (fully developed speckle, no dominant scatterer):

$$\ell(v, b, r) = 2\log(b + r) - \log(2v) + \frac{v^2}{(b + r)^2}\,, \tag{8}$$

or Rice distribution (fully developed speckle with a dominant scatterer):

$$\ell(v, b, r) = \frac{v^2 + s^2}{2b^2} + 2\log(b) - \log[v\,\mathrm{I}_0(v\,s/b^2)]\,. \tag{9}$$

Change detection of strong scatterers:

To detect change in the strong scatterers, we can form the likelihood ratio test:

$$\log \frac{\mathrm{p}(\{v_{t,i}\}|\mathcal{H}_{1b})}{\mathrm{p}(\{v_{t,i}\}|\mathcal{H}_{1a})} \underset{\mathcal{H}_{1a}}{\overset{\mathcal{H}_{1b}}{\gtrless}} \eta\,. \tag{10}$$

For given values of r and b_i, the evaluation of the log-likelihood under hypothesis $\mathcal{H}_{1b}$ requires the estimation of t_c and deciding between the apparition or the disappearance of the scatterer. We therefore consider the generalized likelihood ratio test (GLRT) by replacing unknown values by their maximum likelihood estimates. The GLRT is given by:

$$\mathscr{L}_{1a}(b_i, r) \underset{\mathcal{H}_{1a}}{\overset{\mathcal{H}_{1b}}{\gtrless}} \widehat{\mathscr{L}_{1b}}(b_i, r) + \eta\,, \tag{11}$$

where we define $\widehat{\mathscr{L}_{1b}}(b_i, r)$ by:

$$\widehat{\mathscr{L}_{1b}}(b_i, r) = \min_{t_c} \min\big[\mathscr{L}_{1b}^{\text{app}}(b_i, r, t_c),\, \mathscr{L}_{1b}^{\text{dis}}(b_i, r, t_c)\big]. \tag{12}$$

We thus decide that a change occurred at pixel i, for given values of the background radiometry b_i and of the scatterer radiometry r based on equation (11), with threshold η controlling the false alarm rate (increasing η reduces the false alarm rate).

Detection of strong scatterers:

As for change detection, the detection of strong scatterers is based on the likelihood ratio test

$$\log \frac{\mathrm{p}(\{v_{t,i}\}|\mathcal{H}_1)}{\mathrm{p}(\{v_{t,i}\}|\mathcal{H}_0)} \underset{\mathcal{H}_0}{\overset{\mathcal{H}_1}{\gtrless}} \lambda\,. \tag{13}$$

Since the radiometry of the scatterer must be estimated, we consider the GLRT:

$$\mathscr{L}_0(b_i) \underset{\mathcal{H}_0}{\overset{\mathcal{H}_1}{\gtrless}} \widehat{\mathscr{L}_1}(b_i) + \lambda\,, \tag{14}$$

with

$$\widehat{\mathscr{L}_1}(b_i) = \min_r \min\big[\mathscr{L}_{1a}(b_i, r),\, \widehat{\mathscr{L}_{1b}}(b_i, r) + \eta\big]. \tag{15}$$

Estimation of the radiometry of the background:

The neg-log-likelihood of the background radiometry $\widehat{\mathscr{L}}$ can be derived based on equation (14):

$$\widehat{\mathscr{L}}(b_i) = \min\big[\mathscr{L}_0(b_i),\, \widehat{\mathscr{L}_1}(b_i) + \lambda\big]. \tag{16}$$

In order to enforce that the background radiometries vary smoothly, with possibly some sharp edges, we consider a total variation prior:

$$-\log \mathrm{p}(\boldsymbol{b}) = \mu \sum_{i \sim j} |b_i - b_j| \equiv \mu\,\mathrm{TV}(\boldsymbol{b})\,, \tag{17}$$

where the notation $i \sim j$ denotes pixels i and j that are spatial neighbors.

Estimation of the vector of all m background radiometries in the maximum a posteriori sense requires solving the following hierarchical optimization problem:

$$\hat{\boldsymbol{b}} = \underset{\boldsymbol{b} \in \mathbb{R}^m}{\arg\min} \sum_i \widehat{\mathscr{L}}(b_i) + \mu\,\mathrm{TV}(\boldsymbol{b})\,, \quad \text{s.t.} \quad \boldsymbol{b} \geq 0 \tag{18}$$

where the likelihood term $\widehat{\mathscr{L}}(b_i)$ involves implicit sub-minimizations. By making these sub-minimizations explicit, we get the following constrained optimization problem:

$$
\begin{aligned}
\underset{\substack{\boldsymbol{d}\in\{0,1\}^m \\ \boldsymbol{c}\in\{0,1\}^m \\ \boldsymbol{a}\in\{0,1\}^m \\ \boldsymbol{b}\in\mathbb{R}^m \\ \boldsymbol{r}\in\mathbb{R}^m \\ \boldsymbol{s}\in\mathbb{R}^{mn} \\ \boldsymbol{t_c}\in\{2,\dots,n\}^m}}{\arg\min} \quad & \sum_{i,t} \ell(v_{i,t}, b_i, s_{i,t}) + \lambda \|\boldsymbol{d}\|_0 + \eta \|\boldsymbol{c}\|_0 \\
& \qquad + \mu \, \mathrm{TV}(\boldsymbol{b}) \qquad (19)
\end{aligned}
$$

$$
\begin{aligned}
\text{s.t.} \quad & \forall i,\, \forall t, & (d_i - 1) \cdot s_{i,t} &= 0 \\
& \forall i,\, \forall t, & (c_i - 1) \cdot (s_{i,t} - r_i) &= 0 \\
& \forall i,\, \forall t < t_{ci}, & c_i \cdot a_i \cdot s_{i,t} &= 0 \\
& \forall i,\, \forall t \geq t_{ci}, & c_i \cdot a_i \cdot (s_{i,t} - r_i) &= 0 \\
& \forall i,\, \forall t < t_{ci}, & c_i \cdot (1 - a_i) \cdot (s_{i,t} - r_i) &= 0 \\
& \forall i,\, \forall t \geq t_{ci}, & c_i \cdot (1 - a_i) \cdot s_{i,t} &= 0 \\
& \forall i, & b_i &\geq 0 \\
& \forall i, & r_i &\geq 0
\end{aligned}
$$

where the binary variables d_i, c_i and a_i, respectively indicate whether a strong scatter is present at pixel i, whether its radiometry changes with time, and if the type of change is an "apparition". The constraints enforce that the radiometry of the scatterer component $\boldsymbol{s}$ is 0 in the absence of a strong scatterer, is constant in the absence of change, or is piece-wise constant in case of apparition / disappearance of the scatterer.

Solving this optimization problem seems challenging since it involves a non-convex objective function, nonlinear constraints, and mixed integer and real variables. After quantization of real variables to turn the problem into a purely discrete optimization problem, it can be solved exactly by computing a minimum cut in a 3D graph. Indeed, in the hierarchical optimization form (18), the neg-log-likelihood term $\widehat{\mathscr{L}}(b_i)$ is separable, i.e., it can be evaluated independently for all pixels i for any given values b_i. The optimization problem in (18) is thus the sum of a separable non-convex term and a convex pairwise term. It can then be solved using the graph construct of Ishikawa [6].

Graph construction is represented in figure 1. The graph is composed of several layers, each of them having one node for each of the m pixels of the images. Each layer represents a possible value for the background. Neighboring nodes are connected by pairs of arcs. The source ($\mathcal{S}$) and the sink ($\mathcal{T}$) are also connected to the first and last layers. Each node is connected with a weight of $(\beta_{n+1} - \beta_n)\mu$ for horizontal (black) arcs (see zoom in (1)), $\widehat{\mathscr{L}}(\beta_n)$ for top-down (blue) arcs, and ∞ for bottom-up (red) ones, where $\beta_1, \dots, \beta_m$ are the possible values for the background b.

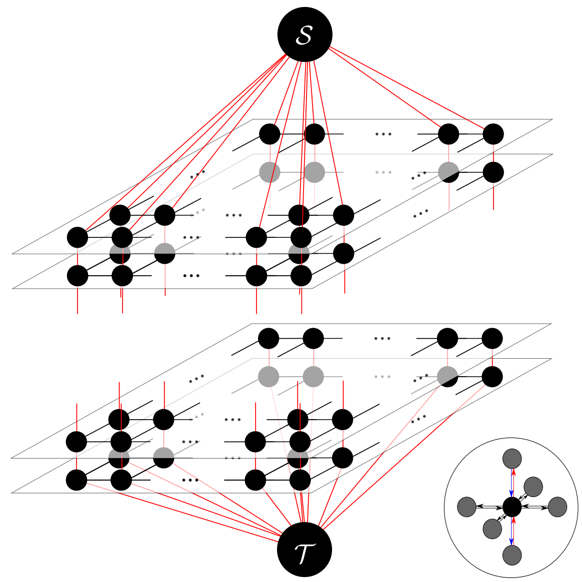

Fig. 1. Graph construction based on [6].

3. RESULTS

To illustrate the proposed method, we ran our algorithm on a multi-temporal series of images acquired by TerraSAR-X of Saint-Gervais (France). The obtained decomposition is shown in figure 2.

A qualitative evaluation of the proposed method is given in figure 3. It features the ROC curve of our method, and compares it to classical change detection algorithm ([7], [8], [9] and [4]). Performances are close to those obtained by [9].

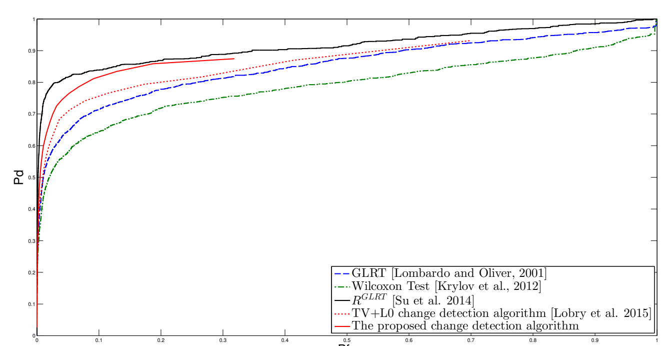

Fig. 3. ROC curve comparing the performances of our algorithm to classical change detection algorithm. Images used are those described in figure 2.

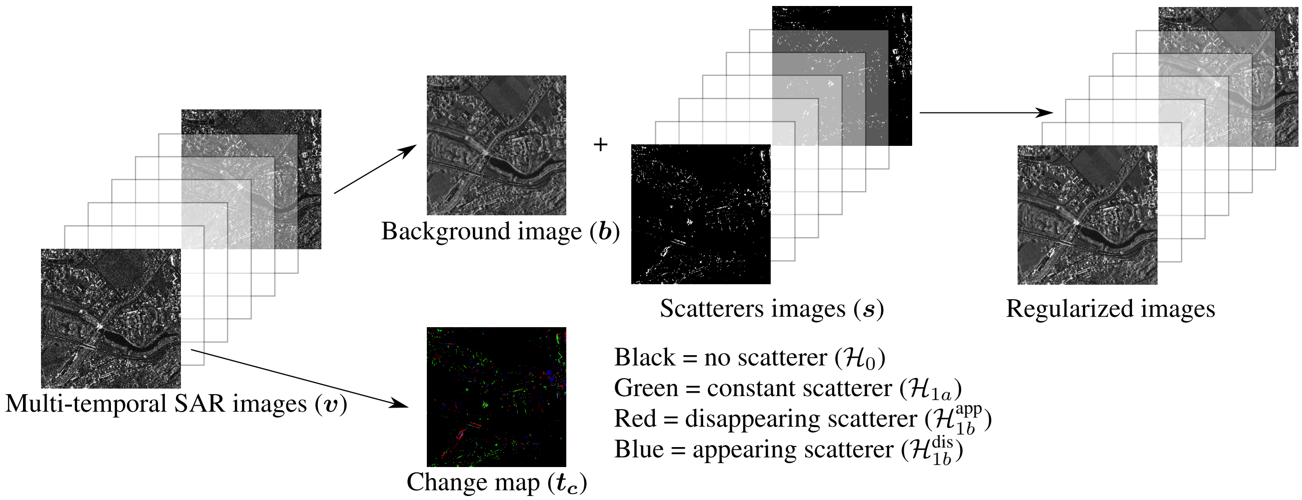

Fig. 2. Results on a multi-temporal series of images acquired by TerraSAR-X of Saint-Gervais, France. The series is composed of 13 images acquired between 05/31/2009 and 25/09/2011. Given a multi-temporal series, the proposed algorithm outputs a background representing the time series, a series of scatterers images and a change map. We can obtain the regularized images at each date by adding the background and the scatterers image of the desired date. In this illustration, we only show the first and last date of the series.

4. CONCLUSION

In this paper, we have introduced a change detection suitable for urban areas method using SAR multi-temporal series of images. This method uses an image decomposition model in order to jointly estimate and regularize background and scatterers, taking into account the fact that these scatterers can be affected by changes.

The proposed model is expressed in a way that allows for an exact optimization using graph-cut techniques and yields results close to the state-of-the-art techniques. A current limitation of this model is that it allows for at most one change per pixel. Future work includes working on more flexible models. Also, we could work on improving the change detection part by controlling the false alarm rate explicitly.

5. REFERENCES

[1] P. Lombardo and T. Pellizzeri, "Maximum likelihood Signal Processing Techniques to detect a Step Pattern of Change in Multitemporal SAR Images," *IEEE Transactions on Geoscience and Remote Sensing*, vol. 40, no. 4, pp. 853–870, April 2002.

[2] M. Horta, N. Mascarenhas, H. Sportouche, N. Seichepine, F. Tupin, and J.-M. Nicolas, "Change detection in multi-temporal HR SAR images: a hypothesis test-based approach," *IGARSS*, pp. 374–377, 2012.

[3] K. Conradsen, A. Nielsen, and H. Skriver, "Change detection in polarimetric SAR data over several time points," *IGARSS*, pp. 4540–4543, 2014.

[4] S. Lobry, L. Denis, and F. Tupin, "Sparse + smooth decomposition models for multi-temporal SAR images," *MultiTemp, Annecy, France*, 2015.

[5] X. Su, C.-A. Deledalle, F. Tupin, and H. Sun, "Two-Step Multitemporal Nonlocal Means for Synthetic Aperture Radar Images," *IEEE Transactions on Geoscience and Remote Sensing*, 2014.

[6] H. Ishikawa, "Exact optimization for Markov random fields with convex priors," *Pattern Analysis and Machine Intelligence, IEEE Transactions on*, vol. 25, no. 10, pp. 1333–1336, 2003.

[7] P. Lombardo and C.J. Oliver, "Maximum likelihood approach to the detection of changes between multitemporal SAR images," *IEEE Proceedings-Radar, Sonar and Navigation*, vol. 148, no. 4, pp. 200–210, 2001.

[8] V. Krylov, G. Moser, A. Voisin, S.B. Serpico, and J. Zerubia, "Change detection with synthetic aperture radar images by Wilcoxon statistic likelihood ratio test," in *IEEE International Conference on Image Processing 2012*, Orlando, United States, Sep 2012.

[9] X. Su, C.-A. Deledalle, F. Tupin, and H. Sun, "NORCAMA: Change Analysis in SAR Time Series by Likelihood Ratio Change Matrix Clustering," *ISPRS Journal of Photogrammetry and Remote Sensing*, pp. 247–261, May 2014.